

Hessian-Aware Pruning and Optimal Neural Implant

Shixing Yu^{*,1}, Zhewei Yao^{*,2}, Amir Gholami^{*,†,2}, Zhen Dong^{*,2}, Michael W. Mahoney², Kurt Keutzer²

¹Peking University, ²University of California, Berkeley

yushixing@pku.edu.cn, {zhewei, amirgh, zhendong, mahoneymw, keutzer}@berkeley.edu

Abstract—Pruning is an effective method to reduce the memory footprint and FLOPs associated with neural network models. However, existing pruning methods often result in significant accuracy degradation for moderate pruning levels. To address this problem, we introduce a new Hessian Aware Pruning (HAP) method which uses second-order sensitivity as a metric for structured pruning. In particular, we use the Hessian trace to find insensitive parameters in the neural network. This is different than magnitude based pruning methods, which prune small weight values. We also propose a new neural implant method, which replaces pruned spatial convolutions with point-wise convolution. We show that this method can improve the accuracy of pruned models while preserving the model size. We test HAP on multiple models (ResNet56, WideResNet32, PreResNet29, VGG16) on CIFAR-10 and (ResNet50) on ImageNet, and we achieve new state-of-the-art results. Specifically, HAP achieves 94.3% accuracy ($< 0.1\%$ degradation) on PreResNet29 (CIFAR-10), with more than 70% of parameters pruned. In comparison to EigenDamage [54], we achieve up to 1.2% higher accuracy with fewer parameters and FLOPs. Moreover, for ResNet50 HAP achieves 75.1% top-1 accuracy (0.5% degradation) on ImageNet, after pruning more than half of the parameters. In comparison to the prior state-of-the-art of HRank [36], we achieve up to 2% higher accuracy with fewer parameters and FLOPs. The framework has been open sourced and available online [2].

I. INTRODUCTION

There has been a significant increase in the computational resources required for Neural Network (NN) training and inference. This is mainly due to larger input sizes (e.g., higher image resolution) as well as larger NN models requiring more computation and significantly larger memory footprint. The slowing down of Moore’s law, along with challenges associated with increasing memory bandwidth, has made it very hard to deploy these models in practice. Often, the inference time and associated power consumption is orders of magnitude higher than acceptable ranges. This has created

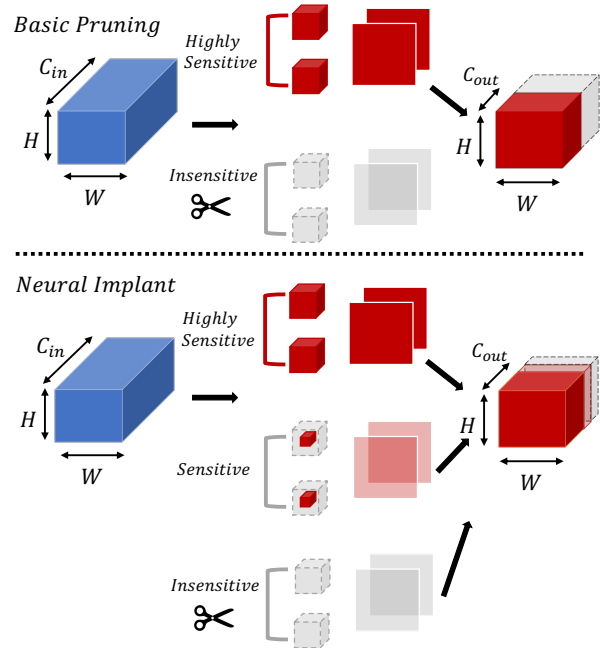


Fig. 1: (Top) The HAP method is a structured pruning method that prunes channels based on their second-order sensitivity. Channels are sorted based on this metric, and only insensitive channels are pruned. (Bottom) In the Neural Implant method, channels with moderate sensitivity levels are replaced with a trainable implant. This approach allows some information to flow from moderately sensitive layers with an implant with few parameters.

a significant burden for many applications, e.g., health care and personalized medicine, which have restrictions on uploading data to cloud servers, and which have to rely on local servers. Other applications include inference on edge devices such as mobile processors, security cameras, and intelligent traffic control systems, all of which require real-time inference. These problems are not limited to edge devices, and state-of-the-art models for applications such as speech recognition, natural language processing, and recommendation systems often cannot be efficiently

^{*}Equal contribution.

[†]Correspondence to: Amir Gholami: amirgh@berkeley.edu

performed even on high-end servers.

A promising approach to address this is pruning [7, 11–15, 17, 32, 33, 35, 40–42, 46, 48, 53–55, 59, 65, 68, 69], where insensitive/extra parameters are removed from the NN. However, an important challenge is determining which parameters are insensitive to the pruning process. A brute-force method is not feasible since one has to test each parameter in the network separately and measure its sensitivity. The seminal work of [33] proposed Optimal Brain Damage (OBD), a second-order based method to determine insensitive parameters. However, this approach requires pruning the parameters one at a time, which is time-consuming. To address this problem, we propose a simple, yet effective, modification of OBD by using the Hessian trace to prune a group of parameters in the NN. We find this approach to be quite effective, and our empirical results show that it can exceed all prior state-of-the-art pruning methods.

In more detail, our contributions are as follows:

- We propose HAP, a Hessian Aware Pruning method that uses a fast second-order metric to find insensitive parameters in a NN model. In particular, we use the average Hessian trace to weight the magnitude of the parameters in the NN. Parameters with large second-order sensitivity remain unpruned, and those with relatively small sensitivity are pruned. In contrast to OBD [33], HAP finds groups of insensitive parameters, which is faster than pruning a single parameter at a time. Details of the HAP method are discussed in Section III.
- We propose a novel neural implant (denoted by HAP+IMPLANT) technique to alleviate accuracy degradation. Specifically, instead of pruning the entire insensitive kernels, we replace them with 1×1 convolutions. These implanted pointwise convolutions are then trained, and this helps boost the accuracy. For details, see Section III-C.
- We show that HAP achieves 94.3% accuracy ($< 0.1\%$ degradation) on PreResNet29 (CIFAR-10), with only 31% parameters left (Figure 3). In comparison to EigenDamage, we achieve up to 1.2% higher accuracy with fewer parameters and FLOPs (Figure 3). Moreover, for ResNet50, HAP achieves 75.1% top-1 accuracy (0.5% degradation) on ImageNet, with only half of the parameters left (Table II). In comparison to prior state-of-the-art HRank [36], HAP achieves up to 2% higher accuracy with fewer parameters and FLOPs (Table II).
- We perform detailed ablation experiments to illustrate the efficacy of our second-order sensitivity metric. In particular, we test HAP performance with a case where

the insensitive layers are chosen randomly (denoted as Random), and reverse-order of HAP (denoted as R-HAP). In all cases, HAP achieves higher accuracy (Table IV).

II. RELATED WORK

Several different approaches have been proposed to make NN models more efficient by making them more compact, faster, and more energy efficient. These efforts could be generally categorized as follows: (i) efficient NN design [23, 24, 27, 44, 51, 66], where the architecture is changed to be both efficient and accurate; (ii) hardware-aware NN design [6, 10, 43, 52, 56, 60], where the NN is adapted to become optimized for a target hardware platform; (iii) quantization [8, 9, 26, 28, 29, 57], where low precision bitwidth is used instead of floating point; (iv) distillation [22, 47, 50, 63], where a teacher model is used to train a compact student model; and (v) pruning [17, 33, 35, 36], where unimportant weights are removed to reduce the amount of computation necessary for inference. Pruning, especially structured pruning, can be an effective way to accelerate inference.

There are mainly two categories of pruning methods: unstructured pruning [7, 34, 49, 58]; and structured pruning [19, 25, 37, 42, 64, 67]. Unstructured pruning prunes out neurons in weight tensors with a pixel-wise granularity. However, this leads to sparse matrix operations which are hard to accelerate and which are typically are memory-bound [5]. This can be addressed with structured pruning, where an entire matrix operation (e.g., an output channel) is removed.

Several different methods have been proposed to determine which parameters to remove. A simple and popular approach is magnitude-based pruning. In this approach, the magnitude of parameters is used as the pruning metric. The assumption here is that small parameters are not important and can be removed. A variant of this approach was used in [39], where the scaling factor of the batch normalization layer is used as the sensitivity metric. In particular, channels with smaller scaling factors (or output values) are considered less important and got pruned. Another variation is proposed by [35], where channel-wise summation over weights is used as the metric. Other methods have been proposed as alternative sensitivity metrics. For instance, [36] uses channel rank as sensitivity metric; [21] uses a LASSO regression based channel selection criteria; and [20] uses the geometric median of the convolutional filters.

An important problem with magnitude-based pruning methods is that parameters with small magnitudes can

actually be quite sensitive. This can be seen using a second-order Taylor series expansion, where the perturbation is dependent on not just the weight magnitude but also the Hessian. In particular, small parameters with large Hessian could in fact be very sensitive, as opposed to large parameters with small Hessian (here, we are using small/large Hessian loosely; the exact metric to measure is given by the second-order perturbation in Eq. 4). This was first shown in the seminal work of OBD [33] where the Hessian diagonal is used as the sensitivity metric. The follow up work of Optimal Brain Surgeon (OBS) [16, 17] used a similar method, but considered off-diagonal Hessian components, and showed a correlation with inverse Hessian. One important challenge with these methods is that pruning has to be performed one parameter at a time. The recent work of [7] extends this to layer-wise pruning in order to reduce the cost of computing Hessian information for one parameter at a time. However, this method can result in unstructured pruning. Another second-order pruning method is EigenDamage [54], where the Gauss-Newton operator is used instead of Hessian. In particular, the authors use Kronecker products to approximate the GN operator. Our findings below show that directly using the full Hessian, without approximation, coupled with our average Hessian trace method, significantly outperforms EigenDamage. In particular, for all of our experiments, we achieved higher accuracy. Furthermore, our method is very simple, it requires few lines of code, and it is quite fast. In particular, our Hessian trace calculation can be performed in three minutes for ResNet50 (on ImageNet).

III. METHODOLOGY

A. Background

Here, we focus on supervised learning tasks, where the nominal goal is to minimize the empirical risk by solving the following optimization problem:

$$L(w) = \frac{1}{N} \sum_{i=1}^N l(x_i, y_i, w), \quad (1)$$

where $w \in \mathbb{R}^n$ is the trainable model parameters, $l(x_i, y_i, w)$ is the loss for the input datum x_i , where y_i is the corresponding label, and N is the training set cardinality. For pruning, we assume that the model is already trained and converged to a local minima which satisfies the first and second-order optimality conditions (that is, the gradient $\nabla_w L(w) = 0$, and the Hessian is Positive Semi-Definite (PSD), $\nabla_w^2 L(w) \succcurlyeq 0$). The problem statement is to prune (remove) as many parameters as possible to reduce the model size and

FLOPs to a target threshold with minimal perturbation to the model.

To motivate our method, we can consider a Taylor series expansion to quantify the effect of this perturbation, when a set of weights are pruned. Let $\Delta w \in \mathbb{R}^n$ denote the perturbation such that the corresponding weights become zero (that is $w + \Delta w = 0$). We denote the corresponding change of loss is represented as ΔL :

$$\Delta L = L(w + \Delta w) - L(w). \quad (2)$$

From a Taylor series expansion, we have:

$$\Delta L = g^T \Delta w + \frac{1}{2} \Delta w^T H \Delta w + O(\|\Delta w\|^3), \quad (3)$$

where $g \in \mathbb{R}^n$ denotes the gradient of loss function L w.r.t. weights w , and $H \in \mathbb{R}^{n \times n}$ is the corresponding Hessian operator (i.e. second-order derivative). For a pretrained neural network that has already converged to a local minimum, we have $g = 0$, and the Hessian is a PSD matrix. As in prior work [17], we assume higher-order terms, e.g., $O(\|\Delta w\|^3)$, in Eq. 3 can be ignored.

The pruning problem is to find the set of weights that result in minimum perturbation to the loss (ΔL). This leads to the following constrained optimization problem:

$$\begin{aligned} \min_{\Delta w} \frac{1}{2} \Delta w^T H \Delta w &= \frac{1}{2} \begin{pmatrix} \Delta w_p \\ \Delta w_l \end{pmatrix}^T \begin{pmatrix} H_{p,p} & H_{p,l} \\ H_{l,p} & H_{l,l} \end{pmatrix} \begin{pmatrix} \Delta w_p \\ \Delta w_l \end{pmatrix}, \\ \text{s.t. } \Delta w_p + w_p &= 0. \end{aligned} \quad (4)$$

Here, we denote the channels that are pruned with p as the subscript, and denote the remaining parameters with l as the subscript. That is, the pruned parameters are denoted as $w_p \in \mathbb{R}^p$, and the remaining parameters are denoted as $w_l \in \mathbb{R}^{n-p}$. Similarly, we use Δw_p and Δw_l to denote the corresponding perturbations. It is not hard to see $\Delta w_p = -w_p$ since p -channels are pruned. Moreover, $H_{l,p}$ denotes the cross Hessian w.r.t. l -channels and p -channels (and similarly $H_{p,p}$ and $H_{l,l}$ are Hessian w.r.t. pruned and unpruned parameters).

We can solve this optimization problem by forming the corresponding Lagrangian and finding its saddle points:

$$\begin{aligned} \mathcal{L} &= \frac{1}{2} \Delta w^T H \Delta w + \lambda^T (\Delta w_p + w_p), \\ \frac{\partial \mathcal{L}}{\partial \Delta w} &= H \Delta w + \begin{pmatrix} \lambda \\ 0 \end{pmatrix} = 0, \\ \begin{pmatrix} H_{p,p} & H_{p,l} \\ H_{l,p} & H_{l,l} \end{pmatrix} \begin{pmatrix} \Delta w_p \\ \Delta w_l \end{pmatrix} + \begin{pmatrix} \lambda \\ 0 \end{pmatrix} &= 0, \end{aligned} \quad (5)$$

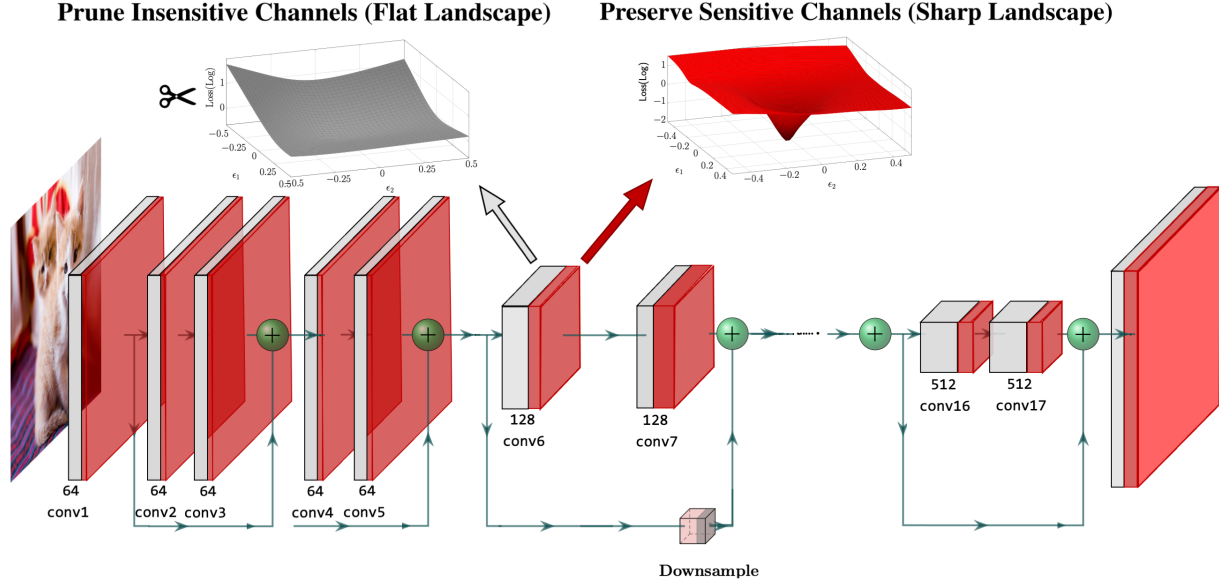


Fig. 2: Illustration of Hessian-Aware Pruning (HAP). Channels are sorted based on their second-order sensitivity (Eq. 11). Insensitive channels are pruned (shown in gray), while sensitive channels are preserved (shown in red).

where $\lambda \in \mathbb{R}^p$ is the Lagrange multiplier, and where the latter equations are derived by taking variations w.r.t. Δw_p . By expanding this equation, we have:

$$H_{p,p}\Delta w_p + H_{p,l}\Delta w_l + \lambda = 0, \quad (6)$$

$$H_{l,p}\Delta w_p + H_{l,l}\Delta w_l = 0. \quad (7)$$

Using the constraint in Eq. 4 and adding it to Eq. 7, we have:

$$\begin{aligned} -H_{l,p}w_p + H_{l,l}\Delta w_l &= 0, \\ \Delta w_l &= H_{l,l}^{-1}H_{l,p}w_p. \end{aligned} \quad (8)$$

This equation gives us the optimal change to the unpruned parameters (w_l), if a pre-selected set of weights is pruned (w_p). Inserting this into Eq. 4 gives us the corresponding perturbation to the loss:

$$\begin{aligned} \frac{1}{2}\Delta w^T H \Delta w &= \frac{1}{2} \begin{pmatrix} \Delta w_p \\ \Delta w_l \end{pmatrix}^T \begin{pmatrix} H_{p,p} & H_{p,l} \\ H_{l,p} & H_{l,l} \end{pmatrix} \begin{pmatrix} \Delta w_p \\ \Delta w_l \end{pmatrix} \\ &= \frac{1}{2}(\Delta w_p^T H_{p,p} \Delta w_p + 2\Delta w_p^T H_{p,l} \Delta w_l \\ &\quad + \Delta w_l^T H_{l,l} \Delta w_l) \\ &= \frac{1}{2}w_p^T (H_{p,p} - H_{p,l}H_{l,l}^{-1}H_{l,p})w_p. \end{aligned} \quad (9)$$

Eq. 9 gives us the perturbation to the loss when a set of parameters w_p is removed. It should be noted that OBS [17] and L-OBS [7], where OBS is applied for each

layer under the assumption of cross-layer independence, is a degenerate case of Eq. 9 for the special case of $w_p \in \mathbb{R}^1$.

B. Hessian-aware Pruning

There are three major disadvantages with OBS. First, computing Eq. 9 requires computing (implicitly) information from the inverse Hessian, $H_{l,l}^{-1}$. This can be costly, both in terms of computations and memory (even when using matrix-free randomized methods). The work of L-OBS [7] attempted to address this challenge by ignoring cross-layer dependencies, but it still requires computing Hessian information (just not Hessian information for the entire network). Second, in both OBS and L-OBS, one has to measure this perturbation for all the parameters separately, and then prune those parameters that result in the smallest perturbation. This has a very high computational cost, especially for deep networks with many parameters. Third, this pruning method results in unstructured pruning, which is undesirable since it leads to sparse matrix operations. These sparse operations are typically memory bound and only result in speed up for extremely high pruning ratios.

One can address the first of these disadvantages (the cost of computing Hessian information) by ignoring all the cross-parameter dependencies, as done in OBD [33].

Here, the Hessian is approximated as a diagonal operator, which results in:

$$\begin{aligned} \frac{1}{2}\Delta w^T H \Delta w &= \frac{1}{2}w_p^T (H_{p,p} - H_{p,l}H_{l,l}^{-1}H_{l,p})w_p. \\ &\approx \frac{1}{2}w_p^T \text{Diag}(H_{p,p})w_p, \end{aligned} \quad (10)$$

where $\text{Diag}(H_{p,p})$ denotes the diagonal elements of $H_{p,p}$. However, the second and third of these disadvantages still remain with OBD.

To address the second and third of these disadvantages, we propose to group the parameters and to compute the corresponding perturbation when that group is pruned, rather than computing the perturbation for every single parameter separately. Note that this can also address the third disadvantage, since pruning a group of parameters (for example parameters in a convolution channel) results in structured pruning. This can be achieved by considering the Hessian as a block diagonal operator, and then approximating each block with a diagonal operator, with Hessian trace as the diagonal entries. In particular, we use the following approximation:

$$\begin{aligned} \frac{1}{2}\Delta w^T H \Delta w &= \frac{1}{2}w_p^T [H^{-1}]_{p,p}^{-1}w_p \\ &\approx \frac{1}{2}w_p^T \frac{\text{Trace}(H_{p,p})}{p}w_p \\ &= \frac{\text{Trace}(H_{p,p})}{2p} \|w_p\|_2^2, \end{aligned} \quad (11)$$

where $\text{Trace}(H_{p,p})$ denotes the trace of the block diagonal Hessian (the corresponding Hessian block for pruned parameters $H_{p,p}$). The Hessian can be computed very efficiently with randomized numerical linear algebra methods, in particular Hutchinson’s method [3, 4, 61, 62]. Importantly, this approach requires computing only the application of the Hessian to a random input vector. This has the same cost as back-propagating the gradient [61, 62]. (Empirically, in our experiments corresponding to ResNet50 on ImageNet, the longest time for computing this trace was three minutes.)

Figure 2 shows a schematic illustration of HAP, where only sensitive layers are pruned, based on their second-order perturbation. In more detail, HAP performs structured pruning by grouping the parameters and approximating the corresponding Hessian as a diagonal operator, with the average Hessian trace of that group as its entries. For a convolutional network, this group can be an output channel. We found that this simple modification leads to a method that exceeds all current pruning results with higher accuracy and lower parameters/FLOPs.

C. Hessian-aware Neural Implant

In the HAP method, we sort the channels from most sensitive to least sensitive (based on Eq. 11). For a target model size or FLOPs budget, one has then to prune among these channels. This approach works well, as long as all these channels are extremely insensitive. However, in practice, some of the sorted channels will exhibit some level of sensitivity. Entirely pruning these channels, and leaving the rest of the sensitive ones unpruned, can lead to sub-optimal performance. We have observed that this is especially the case when the next set of channels has almost the same but slightly higher sensitivity.

We found that a better approach is to avoid entirely pruning these sensitive channels, and instead to add a point-wise convolution as a “neural implant” to them. (This is only applicable to spatial convolution channels.) This allows some information to flow through these relatively sensitive channels. To account for the additional parameters, we can then prune the next set of sensitive channels with a similar implant. This is schematically illustrated in Figure 1. We denote this approach as HAP+IMPLANT. In summary, we use the Hessian sensitivity metric in Eq. 11, and then we apply a neural implant to the most sensitive channels to be pruned (with spatial convolution).

This neural implant approach could be viewed as an interpolative approach, where sensitive layers are partially pruned to preserve some information flow from these layers. We empirically found that this approach is quite effective, especially for moderate pruning ratios.

The neural implant method is essentially a low rank approximation method. Many prior works have investigated low-rank matrix approximation [45]. However, existing methods for NN pruning replace all or part of the model, irrespective of their sensitivity. This is an importantly novelty with our neural implant method; we only replace sensitive parts of the model, quantified through the Hessian in Eq. 11.

IV. RESULTS

A. Experimental Settings

For evaluating the performance of HAP, we conduct experiments for image classification on CIFAR-10 [30] (using ResNet56/WideResNet32/PreResNet29/VGG16) and ImageNet [31] (using ResNet50). For the CIFAR-10 experiments, we use the pretrained WideResNet32 model provided by EigenDamage [54] to ensure a fair comparison with the same baseline. However, we train ResNet56, VGG16, and PreResNet29 from scratch, using

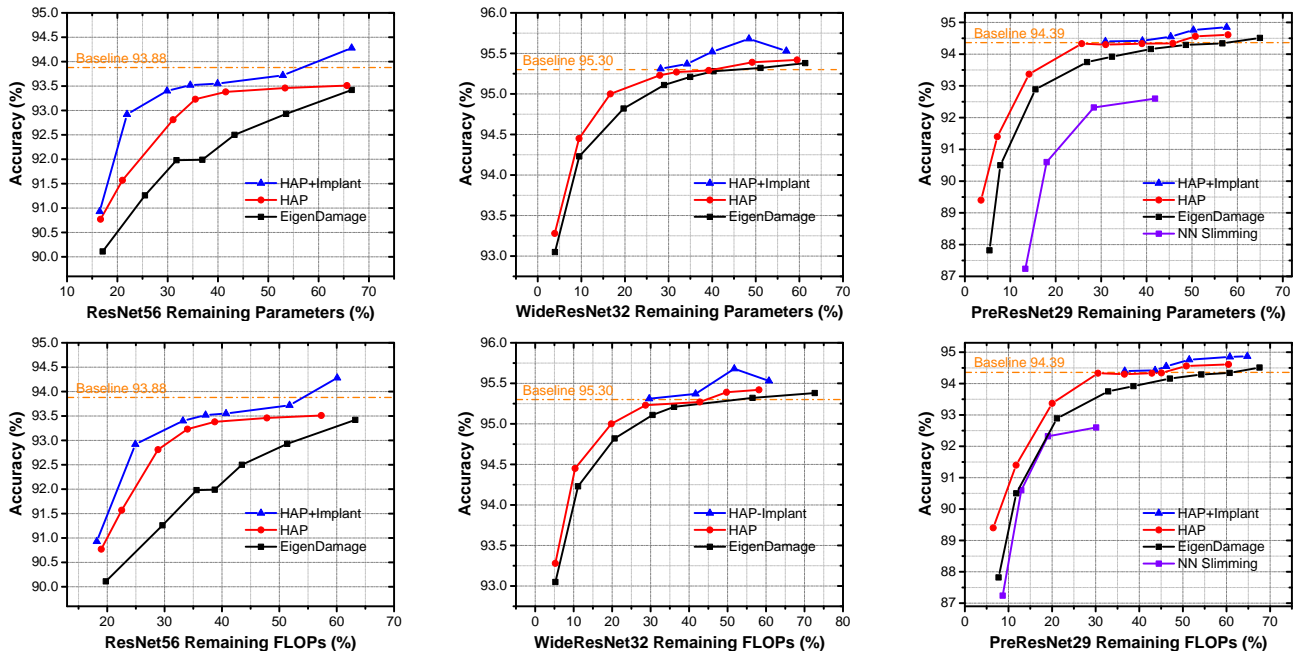


Fig. 3: Comparison of accuracy with different pruning ratios among HAP+IMPLANT, HAP, EigenDamage, and NN Slimming, on the CIFAR-10 dataset, for ResNet56, WideResNet32, and PreResNet29. (Top) Remaining parameters in the network after pruning is used for x-axis. (Bottom) Remaining FLOPs in the network after pruning is used for x-axis. HAP consistently outperforms EigenDamage and NN Slimming, and HAP+IMPLANT boosts performance for moderate pruning ratios.

SGD with momentum, since the pretrained version of these models was not available from EigenDamage. For the ImageNet experiments, we use the pretrained ResNet50 provided by TorchVision [1] library. For all cases, we make sure that the baseline accuracy for these models is comparable to the other pruning methods with which we compare.

We first conduct experiments on a wide range of pruning ratios to compare systematically with other methods. In particular, we compare with the K-FAC Hessian based method of EigenDamage [54] and NN slimming [39], which achieves good pruning accuracy. Furthermore, we compare with L1 [35], ThiNet [42], CP [21], NISP [64], AMC [19], GDP [37], SSS [25], VarP [67], GAL [38], FPGM [20], LFPC [18], and HRank [36]. The metrics we use are validation accuracy, FLOPs, and parameter size. The goal is to achieve higher accuracy with lower FLOPs/parameter size.

B. HAP Results on CIFAR-10

The pruning results of the HAP method for different pruning ratios are illustrated in Figure 3. In particular, we report both the validation accuracy versus remaining parameters in the network, as well as validation accuracy versus the FLOPs of the pruned model. For comparison,

we also plot the performance of EigenDamage [54] and NN slimming [39] for different pruning ratios. For all the points that we compare, HAP achieves higher accuracy, even though its pruned model has fewer parameters and requires fewer FLOPs, as compared to EigenDamage and NN slimming. We generally observe that the difference between HAP and EigenDamage is more noticeable for higher pruning ratios (i.e., fewer remaining parameter). This is expected, since small amounts of pruning does not lead to significant accuracy degradation, while higher pruning ratios are more challenging.

For ResNet56, HAP achieves up to 1.2% better accuracy, as compared to EigenDamage. In particular, when the parameter remaining percentage is around 35% (i.e., 65% of the parameters are pruned), HAP achieves 93.2% accuracy, which is 1.24% higher than EigenDamage, with fewer FLOPs (34.0% versus 38.7% for EigenDamage). We observe a similar trend on WideResNet32, where HAP consistently outperforms EigenDamage.

For PreResNet29, we also compare with NN Slimming [39], to compare with prior reported results on this model. We observe that HAP achieves up to 6% higher accuracy as compared to NN Slimming method, and slightly higher accuracy as compared to EigenDamage. It

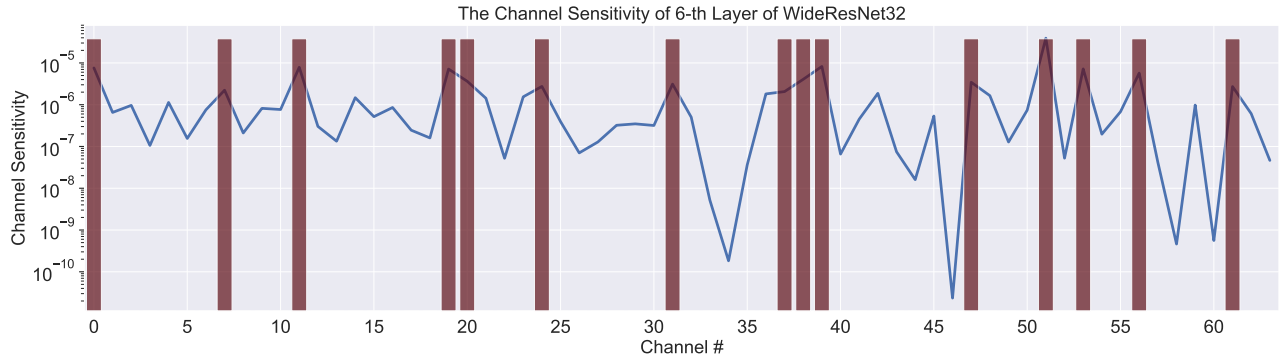


Fig. 4: Illustration of sensitivity of the sixth convolution layer of WideResNet32 (corresponding to 5% parameter remaining in Figure 3). The x-axis denotes the channel number, and the blue line denotes the corresponding second-order sensitivity computed using Eq. 11. The red bar is added to channels that remain unpruned with the HAP method. These correspond to sensitive channels that have large values on the blue line. The corresponding results for ResNet56 and PreResNet29 are presented in Appendix C.

is interesting to note that HAP can keep the accuracy the same as baseline, up to pruning 70% of the parameters (corresponding to 30% remaining parameters in Figure 3).

Furthermore, to illustrate how HAP prunes the model, we plot the second-order sensitivity of different channels in the sixth convolution of WideResNet32 in Figure 4 (blue line). For each channel, we add a binary bar chart which is shown if the channel is not pruned, and vice versa. We can clearly see that layers with lower sensitivity (based on Eq. 11) are pruned. Similar results are seen for other models (see Appendix C).

We also present results on VGG16 and compare with other works in the literature, including GAL [38], HRank [36], and VarP [67], as shown in Table I. Here, we consistently achieve higher accuracy and achieve new state-of-the-art. In particular, HAP with 29.7% FLOPs and 10.1% parameters achieves the highest accuracy (despite using a pretrained model with lower baseline accuracy). Similarly, HAP with 20.3% FLOPs and 5.1% parameters achieves 93.37% accuracy, with less than $2\times$ FLOPs and $3\times$ fewer parameters as compared to HRank in the same block. For extreme pruning, HAP achieves 91.22% accuracy with only 1.6% of the parameters remaining. To the best of our knowledge, this level of aggressive pruning, while maintaining such high accuracy, has not been reported in the literature.

C. NI-HAP Results on CIFAR-10

In Section III-C, we proposed the HAP+IMPLANT method, which replaces spatial convolutions with a pointwise convolution to alleviate the adverse impact of pruning relatively sensitive layers. This replacement

Table I: Comparison between HAP and other pruning methods on CIFAR-10. Here, VGG16 denotes the baseline used in HRank [36], and VGG16-HAP denotes the baseline used by HAP method. As one can see, HAP consistently outperforms other pruning methods, even though its pruned models have fewer parameters (Param.) and FLOPs.

| Method | Acc.(%) | Param.(%) | FLOPs(%) |
|--------------|--------------|-------------|-------------|
| VGG16 | 93.96 | 100.0 | 100.0 |
| VGG16-HAP | 93.88 | 100.0 | 100.0 |
| L1[35] | 93.40 | 36.0 | 65.7 |
| SSS[25] | 93.02 | 26.2 | 58.4 |
| VarP[67] | 93.18 | 26.7 | 60.9 |
| HRank[36] | 93.43 | 17.1 | 46.5 |
| GAL-0.05[38] | 92.03 | 22.4 | 60.4 |
| HRank[36] | 92.34 | 17.9 | 34.7 |
| GAL-0.1[38] | 90.73 | 17.8 | 54.8 |
| HAP | 93.66 | 10.1 | 29.7 |
| HRank[36] | 91.23 | 8.0 | 23.5 |
| HAP | 93.37 | 5.1 | 20.3 |
| HAP | 91.22 | 1.6 | 7.5 |

still reduces the number of parameters for the spatial convolution. For example, for a 3×3 convolutions the number of parameters will reduce by a factor of $9\times$. While this small pointwise convolutional implant is small, it does allow some information to flow from pruned channels.

We repeated the previous experiments with this approach, and we report the results in Figure 3 (blue line).

We observe that HAP+IMPLANT consistently achieves better performance than HAP for both the same parameter size (first row) and the same FLOPs (second row). The performance of the pruned network even exceeds the baseline accuracy for some of the cases.

In particular, for ResNet56, we observe up to 1.5% higher accuracy as compared to HAP, and up to 2% higher accuracy as compared to EigenDamage. Interestingly, for the case with 66.6% parameters remaining (and 60.1% FLOPs remaining), HAP+IMPLANT obtains 94.3% accuracy, which is 0.4% higher than the baseline model. We observe a similar trend for both WideResNet32/PreResNet29, where HAP+IMPLANT consistently performs better than both HAP and EigenDamage.

However, the gains from HAP+IMPLANT diminish for higher pruning ratios (around 20% remaining parameters for ResNet56, and around 30% remaining for WideResNet32/PreResNet29). This is expected, since there is a trade-off associated with adding the neural implant. While the implant helps reduce the information loss from the pruned sensitive channels, it adds additional parameters and forces us to prune additional channels. As the channels are sorted based on their sensitivity (from Eq. 11), this means that we have to prune the next set of sensitive channels. However, if such channels have much higher sensitivity, then they can actually degrade the performance. This is what happens for extreme pruning cases, since most of the remaining parameters will be highly sensitive; and, as such, the gains achieved by preserving the information flow from the relatively less sensitive layers will not be enough. (As future work, one could explore more complex forms of implant to improve this trade-off.)

In addition to parameter percentage, we also compare HAP+IMPLANT results based on remaining FLOPs with other methods reported in the literature. This is shown in Table II. As one can see, with a high remaining FLOPs percentage, HAP+IMPLANT can reach 93.55% accuracy with only 0.33% degradation as compared with the corresponding pretrained baseline model. It should be noted that state-of-the-art methods such as FPGM [20] and LFPC [18] requires 6.4% more FLOPs to reach comparable performance. Moreover, when the target percentage of remaining FLOPs is small, HAP+IMPLANT only incurs 0.96% accuracy degradation as compared with 2.31% for HAP and 2.54% for HRank [36] (with comparable FLOPs and baseline accuracy).

Table II: Comparison of FLOPs and accuracy on CIFAR-10 using ResNet56 for different pruning methods. We report the baseline accuracy used in each work, as well as the corresponding final accuracy after pruning. For ease of comparison, we also report the accuracy drop (Acc. ↓) w.r.t. each baseline. As one can see, HAP and HAP+IMPLANT consistently outperform other work reported in the literature.

| Method | Baseline acc. | Final acc. | Acc. ↓ | FLOPs (%) |
|--------------------|---------------|--------------|-------------|-------------|
| CP[21] | 92.80 | 91.80 | 1.00 | 50.0 |
| AMC[19] | 92.80 | 91.90 | 0.90 | 50.0 |
| FPGM[20] | 93.59 | 93.26 | 0.33 | 47.4 |
| LFPC[18] | 93.59 | 93.24 | 0.35 | 47.1 |
| HAP+IMPLANT | 93.88 | 93.55 | 0.33 | 40.7 |
| GAL-0.8[38] | 93.26 | 90.36 | 2.90 | 39.8 |
| HRank[36] | 93.26 | 90.72 | 2.54 | 25.9 |
| HAP | 93.88 | 91.57 | 2.31 | 21.0 |
| HAP+IMPLANT | 93.88 | 92.92 | 0.96 | 23.9 |

D. HAP Results on ImageNet

We also report the performance of HAP on ImageNet using ResNet50. See Table III. We compare with several previous structured pruning methods including SSS [25], CP [21], ThiNet [42], and HRank [36]. It should be noted that the accuracy of our pretrained baseline is slightly lower than HRank, yet our HAP method still achieves higher accuracy. For instance, in all cases, HAP achieves higher accuracy with smaller number of parameters as compared to all prior work reported on ResNet50. The highest difference corresponds to 34.74% remaining parameters (i.e., pruning 65.26% of parameters), where HAP has 2% higher Top-1 accuracy with 19.26% fewer parameters as compared to HRank (although for fairness our FLOPs are slightly larger). We observe a consistent trend even for high pruning ratios. For example, even with 20.47% remaining parameters, HAP still has more than 2% higher accuracy as compared to HRank. It should also be noted that HAP is quite efficient, and the entire time spent for calculating the Hessian trace was three minutes on a single RTX-6000 GPU.

E. Ablation Study

We also conducted different ablation experiments to study the effectiveness of the second-order based sensitivity metric in HAP. For all the experiments, we use ResNet56 on CIFAR-10.

One of the main components of HAP is the way we sort different channels to be pruned. In particular, this ordering is based on the least sensitive to most sensitive

Table III: Comparison between HAP and state-of-the-art pruning methods on ImageNet. Here, ResNet50 is the baseline used in HRank [36]’s table, while ResNet50-HAP is the baseline used by HAP.

| Method | Top-1 | Param.(%) | FLOPs(%) |
|-------------------|--------------|--------------|--------------|
| ResNet50 | 76.15 | 100.0 | 100.0 |
| ResNet50-HAP | 75.62 | 100.0 | 100.0 |
| SSS-32[25] | 74.18 | 72.94 | 68.95 |
| CP[21] | 72.30 | - | 66.75 |
| GAL-0.5[38] | 71.95 | 83.14 | 56.97 |
| HRank[36] | 74.98 | 63.33 | 56.23 |
| HAP | 75.12 | 55.41 | 66.18 |
| HAP+IMPLANT | 75.36 | 53.74 | 55.49 |
| GDP-0.6[37] | 71.19 | - | 45.97 |
| GDP-0.5[37] | 69.58 | - | 38.39 |
| SSS-26[25] | 71.82 | 61.18 | 56.97 |
| GAL-1[38] | 69.88 | 57.53 | 38.63 |
| GAL-0.5-joint[38] | 71.82 | 75.73 | 44.99 |
| HRank[36] | 71.98 | 54.00 | 37.90 |
| HAP | 74.00 | 34.74 | 40.44 |
| ThiNet-50[42] | 68.42 | 33.96 | 26.89 |
| GAL-1-joint[38] | 69.31 | 40.04 | 27.14 |
| HRank[36] | 69.10 | 32.43 | 23.96 |
| HAP | 71.18 | 20.47 | 32.85 |

Table IV: Ablation study on the sensitivity metric. R-HAP denotes pruning by reversely using sensitivity in HAP. Random is conducted by randomly allocating channel-wise sensitivity.

| Method | Acc. | Param.(%) | FLOPs(%) | Channel |
|-----------|--------------|--------------|--------------|---------|
| R-HAP | 89.77 | 47.48 | 46.98 | 65 |
| Random | 93.12 | 45.60 | 46.68 | 60 |
| Magnitude | 93.29 | 61.82 | 39.29 | 55 |
| HAP | 93.38 | 41.53 | 38.74 | 50 |
| R-HAP | 89.97 | 42.85 | 39.99 | 60 |
| Random | 92.21 | 36.01 | 33.99 | 50 |
| Magnitude | 92.99 | 56.15 | 34.97 | 50 |
| HAP | 93.23 | 35.50 | 33.99 | 45 |
| R-HAP | 88.83 | 27.15 | 30.61 | 50 |
| Random | 90.95 | 29.64 | 31.32 | 40 |
| Magnitude | 92.45 | 47.28 | 28.97 | 42.2 |
| HAP | 92.81 | 31.08 | 28.85 | 40 |
| R-HAP | 88.18 | 23.34 | 28.04 | 45 |
| Random | 90.18 | 25.33 | 25.69 | 30 |
| Magnitude | 91.65 | 38.25 | 22.93 | 35 |
| HAP | 92.06 | 22.05 | 22.86 | 31 |

channels, computed based on Eq. 11. In the first ablation

study, we use the exact reverse order for pruning, and denote this method as R-HAP. The results are shown in Table IV. It can be observed that for all cases R-HAP achieves lower accuracy as compared to HAP (more than 3% for the case with 35.50% remaining parameters). In the second ablation experiment, we use a random order for pruning the layers. The results for this approach is denoted as Random in Table IV. Similar to the previous case, the random ordering achieves consistently lower accuracy as compared to HAP. In addition, its results exhibit a larger variance.

Another important ablation study is to compare the performance of the Hessian-based pruning with the commonly used magnitude based methods, which use variants of $\frac{1}{p}\|w\|_2^2$. In all of the results section our performance is better than magnitude based pruning methods, but here we re-implement the magnitude based methods for further ablation study. The results are reported in Table IV. To make a fair comparison, we set the FLOPs of the model after pruning to be the same for HAP and the magnitude based pruning (and slightly higher for the latter). As the results show, HAP achieves the same accuracy as magnitude based pruning but with much fewer parameters (i.e., higher pruning ratio). In particular, for pruning with 22.53% of FLOPs (last row of Table IV), HAP achieves 92.06% which is almost the same as magnitude based pruning (91.65%). However, HAP achieves this accuracy with only 21.01% of the parameters remaining, as compared to 38.25%, which is quite a significant difference.

V. CONCLUSION

In this work, we proposed HAP, a second-order based pruning method that uses the Hessian trace as a metric to find and prune insensitive parameters in a NN model. We performed extensive empirical tests using multiple NN models. We compared with several prior works, including both the second-order based structured pruning method of EigenDamage, as well as several magnitude-based pruning methods. HAP consistently achieved higher accuracy with fewer parameters. Furthermore, we proposed HAP+IMPLANT, which first performs HAP and then “implants” a small pointwise convolution to pruned sensitive channels. This is performed to avoid complete loss of information from sensitive layers, as measured by our Hessian trace perturbation metric. We found that this simple implant mechanism can boost performance for moderate pruning ratios. Finally, we performed several ablation experiments to study the effectiveness of our second-order sensitivity metric. For

all cases, HAP consistently achieved higher accuracy. We have open sourced our implementation available at [2].

REFERENCES

- [1] Torchvision Library, 2020.
- [2] <https://github.com/yaozhewei/hap.git>, Dec. 2021.
- [3] Haim Avron and Sivan Toledo. Randomized algorithms for estimating the trace of an implicit symmetric positive semi-definite matrix. *Journal of the ACM (JACM)*, 58(2):8, 2011.
- [4] Zhaojun Bai, Gark Fahey, and Gene Golub. Some large-scale matrix computation problems. *Journal of Computational and Applied Mathematics*, 74(1-2):71–89, 1996.
- [5] Aydin Buluc and John R Gilbert. Challenges and advances in parallel sparse matrix-matrix multiplication. In *2008 37th International Conference on Parallel Processing*, pages 503–510. IEEE, 2008.
- [6] Han Cai, Chuang Gan, Tianzhe Wang, Zhekai Zhang, and Song Han. Once-for-all: Train one network and specialize it for efficient deployment. *arXiv preprint arXiv:1908.09791*, 2019.
- [7] Xin Dong, Shangyu Chen, and Sinno Pan. Learning to prune deep neural networks via layer-wise optimal brain surgeon. In *Advances in Neural Information Processing Systems*, pages 4857–4867, 2017.
- [8] Zhen Dong, Zhewei Yao, Daiyaan Arfeen, Amir Gholami, Michael W. Mahoney, and Kurt Keutzer. HAWQ-V2: Hessian aware trace-weighted quantization of neural networks. *Advances in neural information processing systems*, 2020.
- [9] Zhen Dong, Zhewei Yao, Amir Gholami, Michael W. Mahoney, and Kurt Keutzer. HAWQ: Hessian AWare Quantization of neural networks with mixed-precision. In *The IEEE International Conference on Computer Vision (ICCV)*, October 2019.
- [10] Amir Gholami, Kiseok Kwon, Bichen Wu, Zizheng Tai, Xiangyu Yue, Peter Jin, Sicheng Zhao, and Kurt Keutzer. SqueezeNext: Hardware-aware neural network design. *Workshop paper in CVPR*, 2018.
- [11] Luis Guerra, Bohan Zhuang, Ian Reid, and Tom Drummond. Automatic pruning for quantized neural networks. *arXiv preprint arXiv:2002.00523*, 2020.
- [12] Shaopeng Guo, Yujie Wang, Quanquan Li, and Junjie Yan. Dmcp: Differentiable markov channel pruning for neural networks. In *Proceedings of the IEEE/CVF Conference on Computer Vision and Pattern Recognition*, pages 1539–1547, 2020.
- [13] Ghouthi Boukli Hacene, Vincent Gripon, Matthieu Arzel, Nicolas Farrugia, and Yoshua Bengio. Quantized guided pruning for efficient hardware implementations of convolutional neural networks. *arXiv preprint arXiv:1812.11337*, 2018.
- [14] Song Han, Xingyu Liu, Huizi Mao, Jing Pu, Ardavan Pedram, Mark A Horowitz, and William J Dally. Eie: efficient inference engine on compressed deep neural network. *ACM SIGARCH Computer Architecture News*, 44(3):243–254, 2016.
- [15] Song Han, Jeff Pool, John Tran, and William Dally. Learning both weights and connections for efficient neural network. In *Advances in neural information processing systems*, pages 1135–1143, 2015.
- [16] Babak Hassibi and David G Stork. Second order derivatives for network pruning: Optimal brain surgeon. In *Advances in neural information processing systems*, pages 164–171, 1993.
- [17] Babak Hassibi, David G Stork, and Gregory J Wolff. Optimal brain surgeon and general network pruning. In *IEEE international conference on neural networks*, pages 293–299. IEEE, 1993.
- [18] Yang He, Yuhang Ding, Ping Liu, Linchao Zhu, Hanwang Zhang, and Yi Yang. Learning filter pruning criteria for deep convolutional neural networks acceleration. In *Proceedings of the IEEE/CVF Conference on Computer Vision and Pattern Recognition*, pages 2009–2018, 2020.
- [19] Yihui He, Ji Lin, Zhijian Liu, Hanrui Wang, Li-Jia Li, and Song Han. Amc: Automl for model compression and acceleration on mobile devices. In *Proceedings of the European Conference on Computer Vision (ECCV)*, pages 784–800, 2018.
- [20] Yang He, Ping Liu, Ziwei Wang, Zhilan Hu, and Yi Yang. Filter pruning via geometric median for deep convolutional neural networks acceleration. In *Proceedings of the IEEE Conference on Computer Vision and Pattern Recognition*, pages 4340–4349, 2019.
- [21] Yihui He, Xiangyu Zhang, and Jian Sun. Channel pruning for accelerating very deep neural networks. In *Proceedings of the IEEE International Conference on Computer Vision*, pages 1389–1397, 2017.
- [22] Geoffrey Hinton, Oriol Vinyals, and Jeff Dean. Distilling the knowledge in a neural network. *Workshop paper in NIPS*, 2014.
- [23] Andrew Howard, Mark Sandler, Grace Chu, Liang-Chieh Chen, Bo Chen, Mingxing Tan, Weijun Wang, Yukun Zhu, Ruoming Pang, Vijay Vasudevan, et al. Searching for mobilenetv3. In *Proceedings of the IEEE International Conference on Computer Vision*, pages 1314–1324, 2019.
- [24] Andrew G Howard, Menglong Zhu, Bo Chen, Dmitry Kalenichenko, Weijun Wang, Tobias Weyand, Marco Andreetto, and Hartwig Adam. Mobilenets: Efficient convolutional neural networks for mobile vision applications. *arXiv preprint arXiv:1704.04861*, 2017.
- [25] Zehao Huang and Naiyan Wang. Data-driven sparse structure selection for deep neural networks. In *Proceedings of the European conference on computer vision (ECCV)*, pages 304–320, 2018.
- [26] Itay Hubara, Matthieu Courbariaux, Daniel Soudry, Ran El-Yaniv, and Yoshua Bengio. Quantized neural networks: Training neural networks with low precision weights and activations. *The Journal of Machine Learning Research*, 18(1):6869–6898, 2017.
- [27] Forrest N Iandola, Song Han, Matthew W Moskewicz,

- Khalid Ashraf, William J Dally, and Kurt Keutzer. SqueezeNet: AlexNet-level accuracy with 50x fewer parameters and; 0.5 mb model size. *arXiv preprint arXiv:1602.07360*, 2016.
- [28] Benoit Jacob, Skirmantas Kligys, Bo Chen, Menglong Zhu, Matthew Tang, Andrew Howard, Hartwig Adam, and Dmitry Kalenichenko. Quantization and training of neural networks for efficient integer-arithmetic-only inference. In *Proceedings of the IEEE Conference on Computer Vision and Pattern Recognition*, pages 2704–2713, 2018.
- [29] Raghuraman Krishnamoorthi. Quantizing deep convolutional networks for efficient inference: A whitepaper. *arXiv preprint arXiv:1806.08342*, 2018.
- [30] Alex Krizhevsky, Vinod Nair, and Geoffrey Hinton. Cifar-10 (canadian institute for advanced research). URL <http://www.cs.toronto.edu/kriz/cifar.html>, 5, 2010.
- [31] Alex Krizhevsky, Ilya Sutskever, and Geoffrey E Hinton. ImageNet classification with deep convolutional neural networks. In *Advances in neural information processing systems*, pages 1097–1105, 2012.
- [32] Se Jung Kwon, Dongsoo Lee, Byeongwook Kim, Parichay Kapoor, Baeseong Park, and Gu-Yeon Wei. Structured compression by weight encryption for unstructured pruning and quantization. In *Proceedings of the IEEE/CVF Conference on Computer Vision and Pattern Recognition*, pages 1909–1918, 2020.
- [33] Yann LeCun, John S Denker, and Sara A Solla. Optimal brain damage. In *Advances in neural information processing systems*, pages 598–605, 1990.
- [34] Namhoon Lee, Thalaisyasingam Ajanthan, and Philip HS Torr. Snip: Single-shot network pruning based on connection sensitivity. *arXiv preprint arXiv:1810.02340*, 2018.
- [35] Hao Li, Asim Kadav, Igor Durdanovic, Hanan Samet, and Hans Peter Graf. Pruning filters for efficient convnets. *arXiv preprint arXiv:1608.08710*, 2016.
- [36] Mingbao Lin, Rongrong Ji, Yan Wang, Yichen Zhang, Baochang Zhang, Yonghong Tian, and Ling Shao. Hrank: Filter pruning using high-rank feature map. In *Proceedings of the IEEE/CVF Conference on Computer Vision and Pattern Recognition*, pages 1529–1538, 2020.
- [37] Shaohui Lin, Rongrong Ji, Yuchao Li, Yongjian Wu, Feiyue Huang, and Baochang Zhang. Accelerating convolutional networks via global & dynamic filter pruning. In *IJCAI*, pages 2425–2432, 2018.
- [38] Shaohui Lin, Rongrong Ji, Chenqian Yan, Baochang Zhang, Liujuan Cao, Qixiang Ye, Feiyue Huang, and David Doermann. Towards optimal structured cnn pruning via generative adversarial learning. In *Proceedings of the IEEE Conference on Computer Vision and Pattern Recognition*, pages 2790–2799, 2019.
- [39] Zhuang Liu, Jianguo Li, Zhiqiang Shen, Gao Huang, Shoumeng Yan, and Changshui Zhang. Learning efficient convolutional networks through network slimming. In *Proceedings of the IEEE International Conference on Computer Vision*, pages 2736–2744, 2017.
- [40] Zechun Liu, Haoyuan Mu, Xiangyu Zhang, Zichao Guo, Xin Yang, Kwang-Ting Cheng, and Jian Sun. Metapruning: Meta learning for automatic neural network channel pruning. In *Proceedings of the IEEE International Conference on Computer Vision*, pages 3296–3305, 2019.
- [41] Zhuang Liu, Mingjie Sun, Tinghui Zhou, Gao Huang, and Trevor Darrell. Rethinking the value of network pruning. *arXiv preprint arXiv:1810.05270*, 2018.
- [42] Jian-Hao Luo, Jianxin Wu, and Weiyao Lin. Thinet: A filter level pruning method for deep neural network compression. In *Proceedings of the IEEE international conference on computer vision*, pages 5058–5066, 2017.
- [43] Li Lyna Zhang, Yuqing Yang, Yuhang Jiang, Wenwu Zhu, and Yunxin Liu. Fast hardware-aware neural architecture search. In *Proceedings of the IEEE/CVF Conference on Computer Vision and Pattern Recognition Workshops*, pages 692–693, 2020.
- [44] Ningning Ma, Xiangyu Zhang, Hai-Tao Zheng, and Jian Sun. Shufflenet v2: Practical guidelines for efficient cnn architecture design. In *Proceedings of the European Conference on Computer Vision (ECCV)*, pages 116–131, 2018.
- [45] M. W. Mahoney. *Randomized algorithms for matrices and data*. Foundations and Trends in Machine Learning. NOW Publishers, Boston, 2011.
- [46] Huizi Mao, Song Han, Jeff Pool, Wenshuo Li, Xingyu Liu, Yu Wang, and William J Dally. Exploring the regularity of sparse structure in convolutional neural networks. *Workshop paper in CVPR*, 2017.
- [47] Asit Mishra and Debbie Marr. Apprentice: Using knowledge distillation techniques to improve low-precision network accuracy. *arXiv preprint arXiv:1711.05852*, 2017.
- [48] Pavlo Molchanov, Stephen Tyree, Tero Karras, Timo Aila, and Jan Kautz. Pruning convolutional neural networks for resource efficient inference. *arXiv preprint arXiv:1611.06440*, 2016.
- [49] Sejun Park, Jaeho Lee, Sangwoo Mo, and Jinwoo Shin. Lookahead: a far-sighted alternative of magnitude-based pruning. *arXiv preprint arXiv:2002.04809*, 2020.
- [50] Antonio Polino, Razvan Pascanu, and Dan Alistarh. Model compression via distillation and quantization. *arXiv preprint arXiv:1802.05668*, 2018.
- [51] Mark Sandler, Andrew Howard, Menglong Zhu, Andrey Zhmoginov, and Liang-Chieh Chen. MobileNetV2: Inverted residuals and linear bottlenecks. In *Proceedings of the IEEE Conference on Computer Vision and Pattern Recognition*, pages 4510–4520, 2018.
- [52] Mingxing Tan, Bo Chen, Ruoming Pang, Vijay Vasudevan, Mark Sandler, Andrew Howard, and Quoc V Le. Mnasnet: Platform-aware neural architecture search for mobile. In *Proceedings of the IEEE Conference on Computer Vision and Pattern Recognition*, pages 2820–2828, 2019.
- [53] Frederick Tung and Greg Mori. Clip-q: Deep network compression learning by in-parallel pruning-quantization. In *Proceedings of the IEEE Conference on Computer*

- Vision and Pattern Recognition*, pages 7873–7882, 2018.
- [54] Chaoqi Wang, Roger Grosse, Sanja Fidler, and Guodong Zhang. Eigendamage: Structured pruning in the kronecker-factored eigenbasis. *arXiv preprint arXiv:1905.05934*, 2019.
- [55] Ying Wang, Yadong Lu, and Tijmen Blankevoort. Differentiable joint pruning and quantization for hardware efficiency. In *European Conference on Computer Vision*, pages 259–277. Springer, 2020.
- [56] Bichen Wu, Xiaoliang Dai, Peizhao Zhang, Yanghan Wang, Fei Sun, Yiming Wu, Yuandong Tian, Peter Vajda, Yangqing Jia, and Kurt Keutzer. FBNet: Hardware-aware efficient convnet design via differentiable neural architecture search. In *Proceedings of the IEEE Conference on Computer Vision and Pattern Recognition*, pages 10734–10742, 2019.
- [57] Jiaxiang Wu, Cong Leng, Yuhang Wang, Qinghao Hu, and Jian Cheng. Quantized convolutional neural networks for mobile devices. In *Proceedings of the IEEE Conference on Computer Vision and Pattern Recognition*, pages 4820–4828, 2016.
- [58] Xia Xiao, Zigeng Wang, and Sanguthevar Rajasekaran. Autoprune: Automatic network pruning by regularizing auxiliary parameters. In *Advances in Neural Information Processing Systems*, pages 13681–13691, 2019.
- [59] Tien-Ju Yang, Yu-Hsin Chen, and Vivienne Sze. Designing energy-efficient convolutional neural networks using energy-aware pruning. In *Proceedings of the IEEE Conference on Computer Vision and Pattern Recognition*, pages 5687–5695, 2017.
- [60] Tien-Ju Yang, Andrew Howard, Bo Chen, Xiao Zhang, Alec Go, Mark Sandler, Vivienne Sze, and Hartwig Adam. Netadapt: Platform-aware neural network adaptation for mobile applications. In *Proceedings of the European Conference on Computer Vision (ECCV)*, pages 285–300, 2018.
- [61] Zhewei Yao, Amir Gholami, Kurt Keutzer, and Michael W. Mahoney. PyHessian: Neural networks through the lens of the Hessian. *arXiv preprint arXiv:1912.07145*, 2019.
- [62] Zhewei Yao, Amir Gholami, Sheng Shen, Kurt Keutzer, and Michael W Mahoney. Adahessian: An adaptive second order optimizer for machine learning. *arXiv preprint arXiv:2006.00719*, 2020.
- [63] Hongxu Yin, Pavlo Molchanov, Jose M Alvarez, Zhizhong Li, Arun Mallya, Derek Hoiem, Niraj K Jha, and Jan Kautz. Dreaming to distill: Data-free knowledge transfer via deepinversion. In *Proceedings of the IEEE/CVF Conference on Computer Vision and Pattern Recognition*, pages 8715–8724, 2020.
- [64] Ruichi Yu, Ang Li, Chun-Fu Chen, Jui-Hsin Lai, Vlad I Morariu, Xintong Han, Mingfei Gao, Ching-Yung Lin, and Larry S Davis. Nisp: Pruning networks using neuron importance score propagation. In *Proceedings of the IEEE Conference on Computer Vision and Pattern Recognition*, pages 9194–9203, 2018.
- [65] Wenyan Zeng and Raquel Urtasun. Mlprune: Multi-layer pruning for automated neural network compression. 2018.
- [66] Xiangyu Zhang, Xinyu Zhou, Mengxiao Lin, and Jian Sun. Shufflenet: An extremely efficient convolutional neural network for mobile devices. In *Proceedings of the IEEE Conference on Computer Vision and Pattern Recognition*, pages 6848–6856, 2018.
- [67] Chenglong Zhao, Bingbing Ni, Jian Zhang, Qiwei Zhao, Wenjun Zhang, and Qi Tian. Variational convolutional neural network pruning. In *Proceedings of the IEEE Conference on Computer Vision and Pattern Recognition*, pages 2780–2789, 2019.
- [68] Michael Zhu and Suyog Gupta. To prune, or not to prune: exploring the efficacy of pruning for model compression. *arXiv preprint arXiv:1710.01878*, 2017.
- [69] Zhuangwei Zhuang, Mingkui Tan, Bohan Zhuang, Jing Liu, Yong Guo, Qingyao Wu, Junzhou Huang, and Jinhui Zhu. Discrimination-aware channel pruning for deep neural networks. In *Advances in Neural Information Processing Systems*, pages 875–886, 2018.

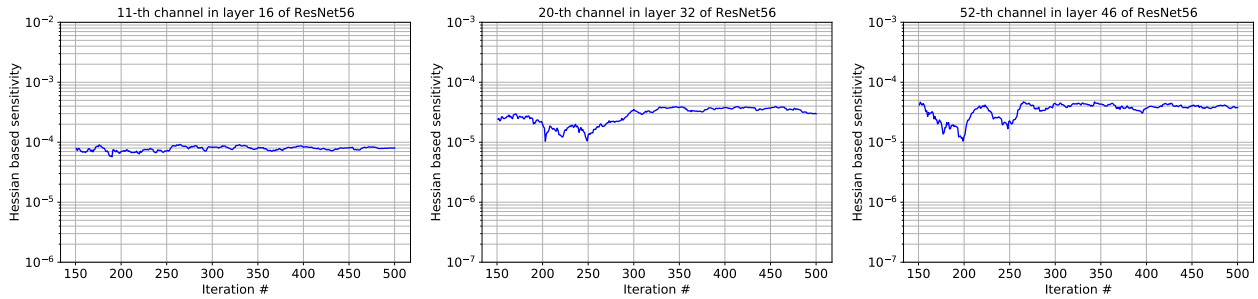


Fig. 5: The convergence of Hessian-based sensitivity throughout the Hutchinson iterations, for different channels of ResNet56. Here, the x-axis is the Hutchinson iteration, and the y-axis is the approximation for the sensitivity corresponding to Eq. 11. As one can see, the approximation converges after about 300 iterations.

APPENDIX

A. Detailed Experimental Setup

Here we present the details of the experiments performed in the paper. For model pretraining on CIFAR-10, we use the same setting as EigenDamage [54]. To finetune the pruned model for performance improvement, we use SGD with momentum 0.9 and train the compressed model for 160 epochs for CIFAR-10 and 120 epochs for ImageNet. The initial learning rate is set as $2e-2$ for CIFAR-10, $1e-3$ for ImageNet, and reduce by one-tenth twice at half and $3/4$ of the full epoch. For CIFAR-10, we use a batch size of 64 and weight decay of $4e-4$, and for ImageNet we use a batch size of 128 and weight decay of $1e-4$. We also set a pruning ratio limit for each layer, following [54].

As for Neural Implant, we select a fixed neural implant ratio of 0.2, meaning that 20% of the pruned 3×3 convolution kernels are replaced by 1×1 convolution kernels.

B. Sensitivity Convergence Results

As discussed in Section III, we compute the sensitivity based on the trace of the Hessian as presented in Eq. 11. This approximation can be computed without explicitly forming the Hessian operator, by using the Hutchinson method [3, 4]. In this approach, the application of the Hessian to a random vector is calculated through backpropagation (similar to how gradient is backpropagated) [61]. In particular, for a given random vector $v \in R^p$ with i.i.d. components, we can show:

$$\text{Tr}(H) = \mathbb{E}[v^T H v]. \quad (12)$$

See [61, 62] for details and discussion. We can directly use this identity to compute the sensitivity in Eq. 11:

$$\frac{\text{Trace}(H_{p,p})}{2p} \|w_p\|_2^2 = \frac{1}{2p} \|w_p\|_2^2 \mathbb{E}[v^T H v]. \quad (13)$$

Here, note that the norm of the parameters is a constant. One can prove that for a PSD operator, this expectation converges to the actual trace. To illustrate this empirically, we have plotted the convergence for this sensitivity metric for different channels of ResNet56. See Figure 5. As one can see, after roughly 300 iterations we get a very good approximation.

C. Additional Results

Here, we show the distribution of pruning for different channels of ResNet56, and PreResNet29. See Figure 6. As one can see, HAP only prunes insensitive channels, and keeps channels with high sensitivity (computed based on Eq. 11).

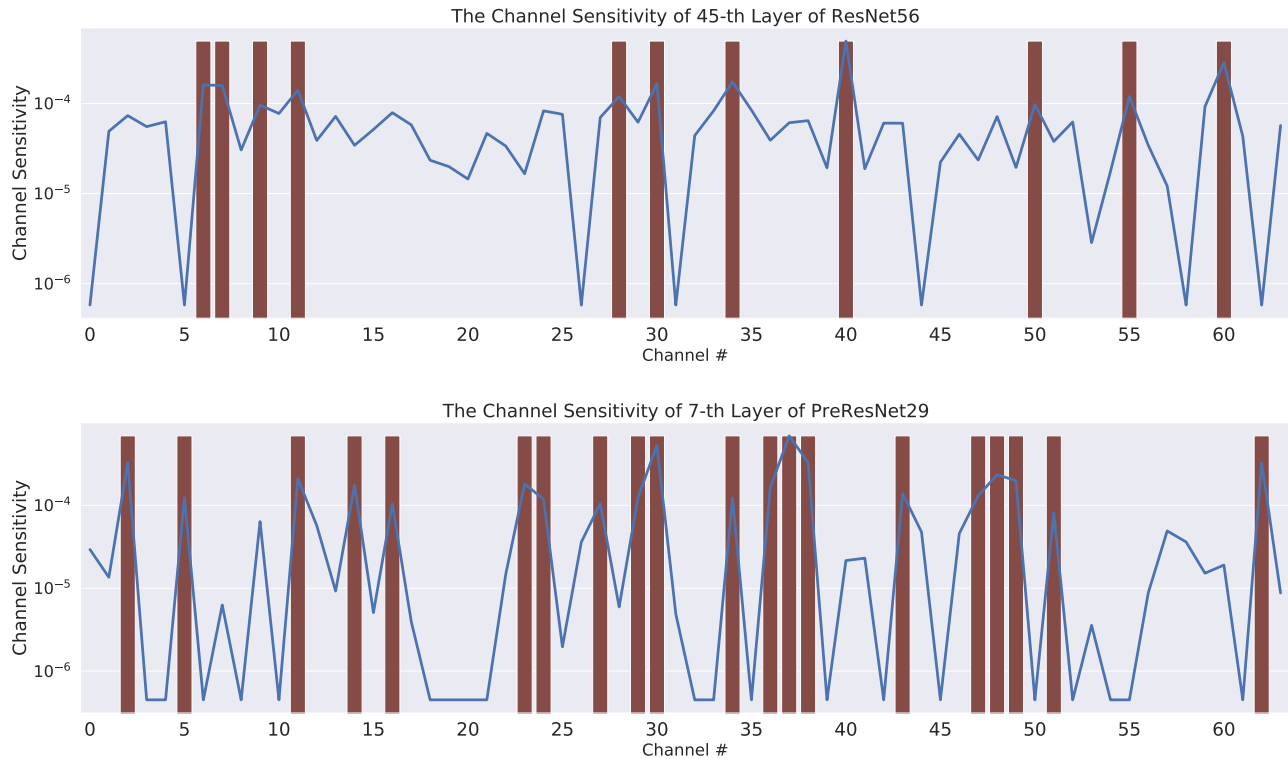


Fig. 6: Illustration of sensitivity of the 45th convolution layer of ResNet56 and the 7th convolution layer of PreResNet29. The x-axis denotes the channel number, and the blue line denotes the corresponding second-order sensitivity computed using Eq. 11. The red bar is added to channels that remain unpruned with the HAP method. As one can see, these correspond to sensitive channels that have large values on the blue line. The corresponding result for WideResNet32 is shown in Figure 4 in main text.